Available online at www.sciencedirect.com
ScienceDirect
Materials Research Bulletin 42 (2007) 1811–1822
Materials Research Bulletin
www.elsevier.com/locate/matresbu

Encapsulation of titanium (IV) silsesquioxane into the NH_4USY zeolite: Preparation, characterization and application

Devaney Ribeiro do Carmo [a,*], Newton Luiz Dias Filho [a], Nelson Ramos Stradiotto [b]

[a] *Faculdade de Engenharia de Ilha Solteira (UNESP), Departamento de Física e Química, Av. Brasil Centro,*
56 CEP 15385-000, Ilha Solteira, SP, Brazil
[b] *Universidade Estadual Paulista, UNESP, Instituto de Química PO Box, Araraquara, SP, Brazil*

Received 27 April 2006; received in revised form 22 November 2006; accepted 1 December 2006
Available online 25 January 2007

Abstract

This work describes the encapsulation of titanium (IV) silsesquioxane into the supercavities of NH_4USY ultra stabilized zeolite, after chemical treatment. The modified zeolite was characterized by Fourier transform infrared spectra, Nuclear magnetic resonance, scanning electronic microscopy, X-ray diffraction and thermogravity. This encapsulated titanium (IV) silsesquioxane can adsorb Azure A chloride after treatment with H_3PO_4, without modifier leaching problems. In an electrochemical study, the cyclic voltammograms of the graphite paste modified electrode, shows two redox couples with formal potential ($E^{0\prime}$) -0.1 V and 0.21 V to I and II redox couples respectively ($v = 700\,\mathrm{mV\,s^{-1}}$; Britton Robinson buffer (B–R) solution, pH 3) *versus* SCE ascribed to a monomer and dimmer of azure. This paper shows the use of ultra stabilized zeolite in the electrochemical field as host for molecules with nanometric dimensions.

Keywords: A. Nanostructures; A. Surfaces; B. Chemical synthesis; C. Infrared spectroscopy; C. Nuclear magnetic resonance (NMR)

---

1. Introduction

The term silsesquioxane [1] is usually related to all structures showing the empiric formula $(RSiO_{1.5})_n$, where R may be a hydrogen or some organic group such as alkyl, methyl, aryl, vinyl, phenyl or any organofunctional derivative from these organic groups. Each silicon atom is, on average, connected to 1.5 oxygen atoms and to an R group (hydrocarbon). When $n = 4$, 6, 8, 10; ($n \geq 4$), the resulting compounds are called polyhedral oligomeric silsesquioxanes [2] (POSS), and if n is an undefined number, this compound is simply called polysilsesquioxane.

In the last decade, the interaction of elements from group 1A and the transition metals with silanols groups [2–6] with silsesquioxane of incomplete condensation have been published. Such complexes are able to mimic the major heterogeneous characteristics of the inorganic-modified silicon with transition metals. The most prominent characteristics include electro-donator sites [6], interactions with donator neighboring oxygen that contribute to the clusters stability [7,8], and to the defined orientation of hydroxyl groups at the surface [9], which shows the selectivity in which the reagent reacts on the surface.

---

* Corresponding author. Tel.: +55 18 3743 1076; fax: +55 18 3742 4868.
E-mail address: docarmo@dfq.feis.unesp.br (D.R. do Carmo).

0025-5408/$ – see front matter © 2006 Elsevier Ltd. All rights reserved.
doi:10.1016/j.materresbull.2006.12.001

There are several silsesquioxane applications and they become wider when used as precursory on the formation of organic or inorganic hybrid materials (ormosils or osmocers) [1]. The most common applications are those related to technological significance, such as: additives [10–13] (crossed bonds agents and thermal and viscosity modifiers); polymers [14] (medical materials, advanced plastics and elastomeric resins); liquid crystals [15]; electroactive films [16]; biosensors [17] precursory for silicon interface [6]; glass and ceramic matrixes [18] and especially, homogenous and heterogeneous catalysts [19].

Recent studies, where spectroscopic techniques were employed [19], showed that the titanium (IV) silsesquioxane is strongly adsorbed by the molecular sieve ‘‘Mobil Composition of Mater-41’’ (MCM-41), and effectively applied in the olephine epoxidation reactions in catalysis, especially when the Si/Al relation is the highest possible. The strong interaction occurs between the ancillary cyclohexyl ligands of the complex and the MCM-41 pore wall. In the present report, the aluminum extraction was necessary in order to preserve and to guarantee the metallic center accessibility to the olephines epoxidations, hence avoiding its lixiviation.

More recently, Smet et al. [20] found that when immobilization is performed through chemical bonding, in other words, the MCM-41 silicon is firstly performed (functionalized) with 3-(glicidiloxipropyl) trimetoxisilane and then react it with $Ti(OBu)_4$, the extraction of the aluminum contained in the MCM-41 silicon is no longer required.

Through those similarities, the present work aims to synthesize and to study the encapsulation of titanium (IV) silsesquioxane into the supercavities of NH_4USY ultra stabilized zeolite. Currently, emphasis is being placed on the preparation of zeolites containing pores of several dimensions. However, modifications of such zeolites are not commonly described. In this study, the immobilization of the Ti (IV) into the NH_4USY zeolite cavity in tetrahydrofurane (THF) medium is emphasized. We will demonstrate, through the characterization of this material by physical and chemical techniques, that the titanium (IV) silsesquioxane structure remained unchanged.

The coordination of metals with electronic configuration d^0 into a silsesquioxane structure tends to generate an electrophilic metallic center. The silsesquioxane structure ($Si_8O_{12}^-$) is an electron acceptor in such way that it has been compared to the group CF_3^- [21]. Such characteristics, in addition to the high NH_4USY zeolite porosity and surface area, are of great importance to the employment of heterogeneous catalysis and in the construction of electrodes, especially concerning its use in electroanalysis [22]. As a means of application in these new hybrid materials, Azure A chloride, a phenothyazine compound, was adsorbed into modified zeolite with silsesquioxane.

2. Experimental

2.1. Reagents and solutions

All reagents and solvents were of analytical grade (Alpha Aesar, Merck or Aldrich) and were used as purchased. All solutions and supporting electrolytes were prepared using Milli-Q water. The electrochemical behavior of modified zolite with Azure A was placed in a 0.1 mol L^{-1} Britton Robinson buffer (B–R). solution. The composition of the B–R solution is 1 L of water containing 3.92 g H_3PO_4 (2.71 mL of 85% H_3PO_4) 2.40 g CH_3COOH (2.36 mL of CH_3COOH) and 2.47 g H_3BO_3. The 0.1 mol L^{-1} NaOH solution was used to adjust the different pHs.

2.2. HUSY zeolite treatment

Modification of the HUSY zeolite (EZ-190P, from Engelhard Corporation Catalysts for Industry, $Si/Al_{rede} = 11$ and $Si/Al_{global} = 6.1$) in the NH_4USY form was initially performed. For that purpose, a solution containing 72.0 g of NH_4NO_3 dissolved into an Erlenmeyer flask containing 300 mL of deionized water was prepared. About 4.23 g of HUSY zeolite was dispersed in this solution, thus initiating the ionic exchange process under agitation for 24 h at room temperature. This process was repeated two more times. After the 1st and the 2nd exchanges, the sample was filtered and washed with 600 mL of deionized water and after the 3rd exchange, the sample was filtered and washed with 1200 mL of deionized water. This sample was then dried in a vacuum dryer and afterwards kept in a dryer containing NH_4Cl saturated solution.

2.3. Preparation and encapsulation of $[(c\text{-hexyl})_7Si_7O_{12}Ti(OPr^i)]$ into the NH_4USY zeolite

The titanium silsesquioxane (IV) was prepared from trisilanolcyclohexyl-POSS ($R_7Si_7O_{12}H_3$; R = c-C_6H_{11}) and titanium isopropoxide ($Ti(O^iPr)_4$) using the corner capping reaction [3] (see Fig. 1).

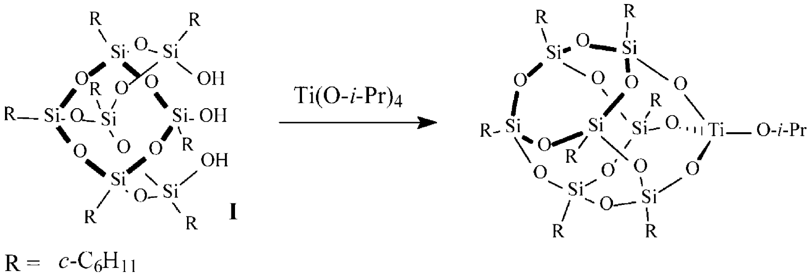

Fig. 1. Scheme of the [(*c*-hexyl)$_7$Si$_7$O$_{12}$Ti(OPr^i)] preparation.

In a typical adsorption experiment the 25 ml of 10^{-3} mol L^{-1} solution of titanium silsesquioxane in tetrahydrofurane (THF) was added at 2 g of NH$_4$USY zeolite and stirred for 24 h. The adsorbed zeolite was separated and washed with solvent (3 × 20 mL) and air-dried at 80 °C for 24 h. The amount of titanium (0.821 mmol Ti/g per gramme of zeolite) was determined using X-ray fluorescence.

2.4. Reaction of modified zeolite with Azure A chloride

First, the modified zeolite was treated with a solution of H$_3$PO$_4$ in a mixture with ethanol to activate the titanium silsesquioxane Bronsted site and to miniminize the hydrofobic nature of titanium silsesquioxane, respectively. The procedure was as follows: In a solution containing 13.0 mL of H$_3$PO$_4$ (0.001 mol L^{-1}) and 7.0 mL of ethanol and 3.2 mg of Azure A chloride (C$_{14}$H$_{14}$ClN$_3$S), 500 mg of modified zeolite were added. After addition of the modified zeolite, the solid phase was stirred for 5 h. The resulting blue material, called ATZ, was collected and washed with 1 L of solution containing H$_3$PO$_4$ 0.001 mol L^{-1} mixed with ethanol (35%) and then dried at room temperature. Fig. 2 shows the scheme of the ATZ preparation.

2.5. Preparation of chemically modified carbon paste electrodes

The chemically modified carbon paste electrodes were prepared by mixing the modified zeolite (ATZ, 20 mg), graphite powder (80 mg), and nujol oil (25 μL). The electrode body was fabricated from a glass tube of i.d. 3 mm and height of 14 cm, containing graphite paste. A copper wire was inserted through the opposite end to establish electrical contact. After the mixture had been homogenized, the modified paste was carefully positioned on the tube tip to avoid

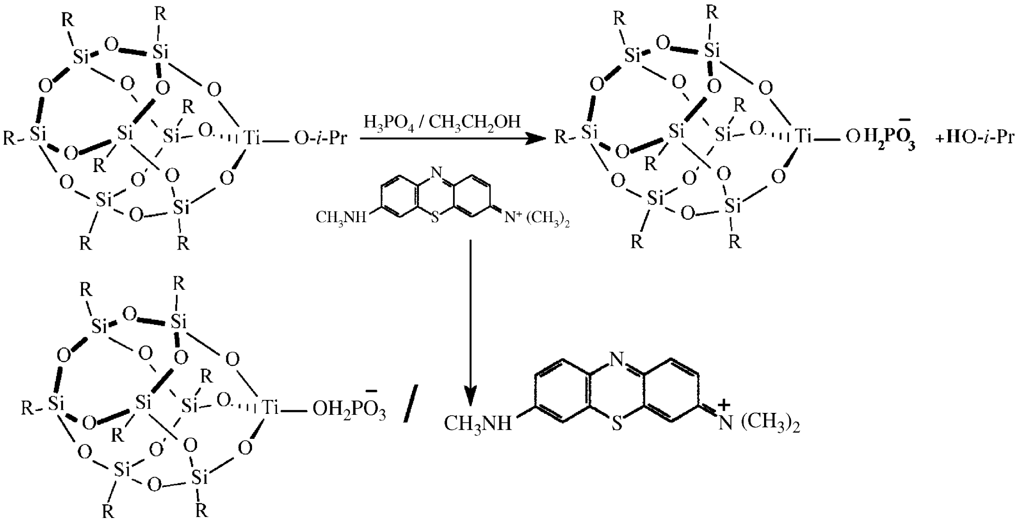

Fig. 2. Scheme of the ATZ preparation.

possible air gaps, which often enhances electrode resistance. The external surface of the electrode was smoothed on soft paper. A new surface can be produced by scraping out the old surface and replacing the carbon paste.

3. Techniques

3.1. Fourier transform infrared spectra

Fourier transform infrared spectra were recorded on a Nicolet 5DXB FT-IR 300 spectrometer. Approximately 600 mg of KBr was ground in a mortar with a pestle, and sufficient solid sample was ground with KBr to make a 1 wt% mixture to produce KBr pellets. After the sample was loaded, the sample chamber was purged with nitrogen for a minimum of 10 min prior to data collecting. A minimum of 32 scans was collected for each sample at a resolution of 4 cm^{-1}.

3.2. Nuclear magnetic resonance analyses (NMR)

All solid state analyses of ^{29}Si (59.5 MHz) and ^{13}C NMR (75.4 MHz) were recorded on a Varian INOVA 300 spectrometer. The samples were packed in zirconia rotors and spun at the magic angle at 4500 Hz, a relaxation delay of 10.0 and 6.0 s for ^{29}Si and ^{13}C, respectively. All chemical shifts are reported in parts per million ppm (δ) with reference to external tetramethylsilane (TMS).

3.3. Microscopy

The scanning electronic microscopy of the materials were obtained using a JEOL JSM T-300 microscope. The samples were adhered over aluminum holders and covered with a thin layer (20–30 nm) of gold in Sputter Coater Bal-Tec SCD-050.

3.4. X-ray diffraction

The X-ray diffraction patterns (XRD) were obtained using a Siemens D 5000 diffractometer with Cu Kα radiation, submitted to 40 kV, 30 mA, $0.05^\circ\ \mathrm{s}^{-1}$ and exposed to radiation from 5 up to 30° (2θ).

3.5. Thermal analyses

Thermogravimetry was performed with a Mettler 181 thermoanalyser. The samples (5–10 mg) were placed in platinum samples holders. The runs were performed under air stream (50 ml/min). The samples were heated at a ramp of 10 °C/min to the final temperature of 1000 °C.

3.6. Electrochemical measurements

Cyclic voltammograms were performed using the Auto Lab (PGSTAT 30-Eco chemie). The three electrodes system used in these studies consisted of a modified working electrode (graphite paste electrode; internal diameter $((\phi) = 0.5$ mm), a saturated calomel electrode (SCE) reference electrode, and a platinum wire as the auxiliary electrode.

4. Results and discussion

The Y zeolite, corresponds to a system established through the union of supercavities, also called α cavities, which are established by 12 oxygen atoms rings, whose diameters range from 0.74 to 0.8 nm [23–24]. The Y zeolite also shows a channel system that is established through the union of sodalite and α supercavities, which enters through an opening generated by six oxygen atoms of a 0.22 nm diameter. Due to the small size of the pore, the second canal system is inaccessible to inorganic and organic molecules; however, the first one is sufficiently large so as to allow access to the majority of molecules used as reagents.

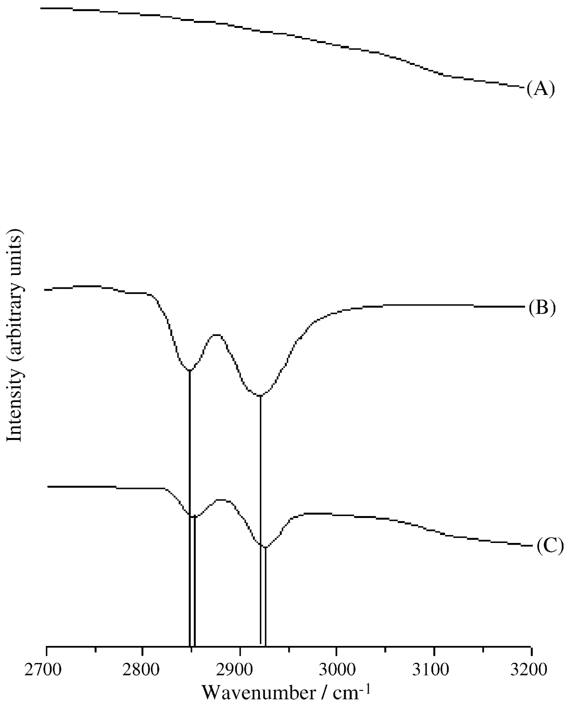

Fig. 3. Fourier transform infrared spectra of: (A) zeolite; (B) titanium; (IV) silsesquioxane; (C) modified zeolite with titanium; (IV) silsesquioxane.

The infrared absorption spectrum (FT-IR) of the zeolite and the pure and adsorbed titanium (IV) silsesquioxane at the zeolite supercavities are illustraded in Fig. 3. For a more detailed discussion concerning the spectrum we divided into two different regions: the first one from 400 to 1500 cm^{-1} and the second one from 2700 to 3200 cm^{-1}. The first region shows absorption bands typical for silica skeleton as well as for the cyclohexyl ligands, found at 1448 cm^{-1} typical from the free complex $[(c\text{-hexyl})_7Si_7O_{12}Ti(OPr^i)]$. The main vibration bands are summarized in Table 1. The typical absorption bands for the $[(c\text{-hexyl})_7Si_7O_{12}Ti(OPr^i)]$ complex is easily recognized after the immobilization in the NH_4USY zeolite (Fig. 3B and C), once there is no absorption of the NH_4USY zeolite (Fig. 3A) at the selected region (2700–3200 cm^{-1}).

In the region from 2700 to 3200 cm^{-1}, some characteristics of the C–H stretching vibrations of the ancillary cyclohexyl ligands for the titanium (IV) silsesquioxane were observed. In this region, two important bands must be considered for discussion purposes: (a) the symmetric CH_2 stretching vibration for the cyclohexyl ligands, found at 2844 cm^{-1}; (b) the asymmetric CH_2 stretching vibration found at 2918 cm^{-1} for the adsorbed material. After the zeolite modification with the Ti(IV) silsesquioxane, some interesting changes were noted. A clear shift was observed when comparing the spectrum of the free complex and adsorbed complex in the zeolite, both bands (symmetric and asymmetric CH_2 stretching vibrations) shifted about 10 cm^{-1} to a higher frequency (see Table 1 and Fig. 3). Therefore,

Table 1
Main FT-IR vibrations of titanium (IV) silsesquioxane complex free and adsorbed inside zeolite NH_4USY

Main vibrations	$[(c\text{-hexyl})_7Si_7O_9Ti(OPr^i)]$ (cm^{-1})	$[(c\text{-hexyl})_7Si_7O_9Ti(OPr^i)]$ adsorbed inside NH_4USY (cm^{-1})
Si–O–Si (stretching)	895	906
C–C (stretching)	925	946
H–C–H “scissors”	1448	1448
Symmetric CH_2 stretching	2844	2854
Asymmetric CH_2 stretching	2918	2927

Main fourier transform infrared spectra vibrations of titanium (IV) silsesquioxane complex free and adsorbed inside zeolite NH_4USY.

this observed shift, of the CH_2 stretching vibrations, seems to be exclusively related to the silsesquioxane adsorption in the NH_4USY zeolite supercavities.

In this study, as shown in Table 1, some vibrations were not affected by the adsorption process once in the spectrum of adsorbed complex, some vibrations remain at the same position before and after the modification of $[(c\text{-hexyl})_7Si_7O_{12}Ti(OPr^i)]$ inside NH_4USY zeolite supercavities.

The shift observed for the CH_2 stretching vibrations was attributed to the reduced space available for the CH_2 stretching vibration arising from a contrained configuration of the cyclohexyl units that resulted from the strong adsorption of the titanium (IV) silsesquioxane adsorption in the NH_4USY zeolite cavities. The displacement frequency into higher energy was also described by Frunza et al. [25], in this case, the adsorption was purely physical, meaning, no chemical interaction was involved.

Figs. 4 and 5 show the spectrum of the ^{29}Si and ^{13}C nuclear magnetic resonance at solid state (MAS NMR) for all studied materials, respectively.

After the encapsulation of the titanium (IV) silsesquioxane into the NH_4USY zeolite (Fig. 4C), two distinct regions were observed in the ^{29}Si NMR spectrum: the first region containing low intensity signs with chemical shifts (δ) of −67.48 and −69.60 ppm, attributed to the silanol $T(O_{3/2}Si\text{-C-hexil})$[26], that is similarly observed for the free titanium (IV) silsesquioxane (relative intensity of 1:3), according to Fig. 4B, and the second region containing peaks with a chemical shift of −102.8 and −108.14 ppm, attributed to the Q^3 and Q^4 sites present in the NH_4USY zeolite.

Fig. 5 represents the spectrum ^{13}C NMR from the free (A) and immobilized in the NH_4USY zeolite pores (B), respectively. The spectrum of immobilized precursory in the NH_4USY zeolite pores (Fig. 13B) showed three resonances with a chemical shift of 25.99, 27.98, and uncommonly of 68.48 ppm. The first two peaks are related to the *ipso* carbon (i.e., those that bond to a silicon atom, from the others pertaining to the cyclohexyl groups) and to the CH_2 groups from the cyclohexyl groups, which generally occur at different regions (δ 22–25 ppm) from the remaining groups CH_2 (26.5–30.0 ppm). Preliminarily, the chemical shift verified at 68.5 ppm was experimentally attributed to the cyclohexyl groups attached to the zeolite supercavity, as verified by the FT-IR. This peak was not verified in either the titanium (IV) silsesquioxane precursory (Fig. 5A) or in the NH_4USY zeolite (Fig. 5C).

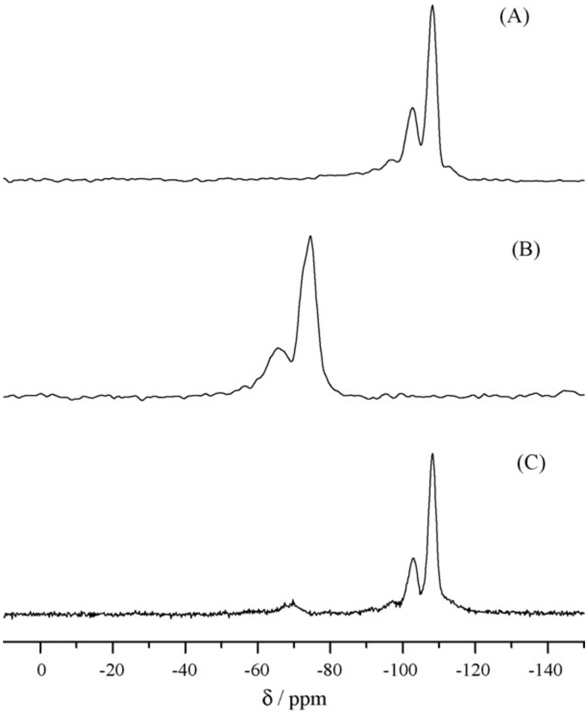

Fig. 4. ^{29}Si nuclear magnetic resonance solid state for: (A) zeolite; (B) titanium; (IV) silsesquioxane; (C) modified zeolite with titanium; (IV) silsesquioxane.

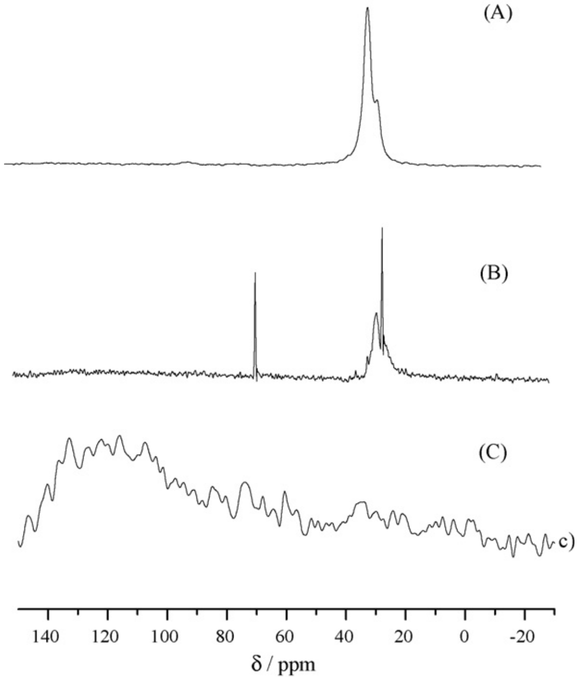

Fig. 5. ^{13}C Nuclear magnetic resonance solid state for: (A) titanium; (IV) silsesquioxane; (B) modified zeolite with titanium; (IV) silsesquioxane; (C) zeolite.

The scanning electron microscopy (SEM) of the NH_4USY zeolite shows perfectly dispersed polyhedral microparticles with relative size < 5 μm. After the adsorption of the titanium (IV) silsesquioxane inside the supercage of zeolite, the particles join to form aggregates with sizes up to 6 μm.

The effect of ([(*c*-hexyl)$_7$Si$_7$O$_{12}$Ti(OPr^i)] in the NH_4USY zeolite crystallinity was also verified through X-ray diffraction (XRD). Fig. 6 illustrates the diffractograms obtained before (A) and after (C) the NH_4USY zeolite modification. Two aspects could be emphasized from these results after the modification process (Fig. 6C): the generation of a new diffraction 2θ to 6.98°, existing in the silsesquioxane precursory (Fig. 6B) and the reduction of the diffraction peak intensity at 2θ to 10.3°, exhibited by zeolite (Fig. 6A). Such observations clearly show that the ([(*c*-hexyl)$_7$Si$_7$O$_9$Ti(OPr^i)] is occluded in the supercavity cavities of the NH_4USY.

The adsorption effect of ([(*c*-hexyl)$_7$Si$_7$O$_{12}$Ti(OPr^i)] inside the supercavity of the NH_4USY zeolite porosity were interpreted through nitrogen adsorption and desorption isotherms, according to the method proposed by Brunauer, Emmett, and Teller (BET), inasmuch as this method is the most commonly employed for the establishment of the superficial area in porous solid materials [27]. Table 2 lists the main surface characteristics of the free and encapsulated NH_4USY zeolite with ([(*c*-hexyl)$_7$Si$_7$O$_{12}$Ti(OPr^i)].

Fig. 7 illustrates a comparison of the isotherms behaviors of NH_4USY zeolite (A) and zeolite containing ([(*c*-hexil)$_7$Si$_7$O$_9$Ti(OPr^i)] (B) in its cavities, respectively. The adsorption and desorption isotherms obtained for the NH_4USY zeolite before and after the modification have behaved as a type IV adsorption, which posses a distinct hysteresis loop. The hysteresis loop is evidenced at relative pressure of 0.45 (P/P^0), according to the IUPAC [28].

The initial dealumination (chemical treatment) process results in enlargement of the pores diameter [29], permitting accessibility of the Ti(IV) inside the supercavity. A decrease (∼20%) on the surface area after the adsorption was observed. The zeolite porosity, micropore volume and external area, after the modification, also decrease.

Thermogravimetrical studies enable the presence of Ti(IV) silsesquioxane to be shown in the zeolite pores. As Fig. 8 (A) illustrates, one single stage of air decomposition (302–622 °C) was verified for NH_4USY zeolite.

Different thermogravimetrical behaviors were verified for the ([(*c*-hexyl)$_7$Si$_7$O$_9$Ti(OPr^i)] adsorbed into the NH_4USY zeolite, for synthetic air atmosphere environment, according to Fig. 8(B). In air atmosphere, the NH_4USY zeolite basically showed a single decomposition stage, which starts at 82 °C, reaching up to 300 °C, with a mass loss of

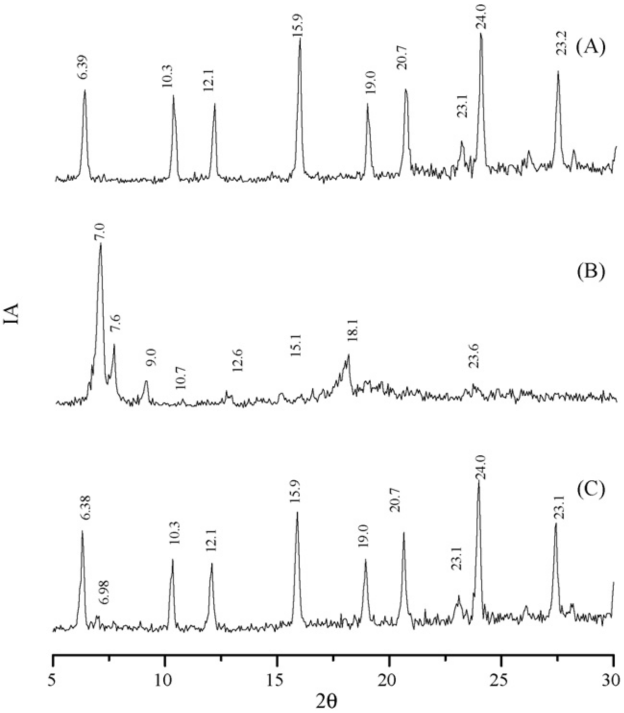

Fig. 6. X-ray powder diffraction of: (A) zeolite; (B) titanium; (IV) silsesquioxane; (C) modified zeolite with titanium; (IV) silsesquioxane.

17.6% NH_4USY. After immobilization of the ($[(c\text{-hexyl})_7Si_7O_{12}Ti(OPr^i)]$ in its cavities, two decomposition stages were observed; the first one with mass loss of 13.7% up to 350 °C (attributed to the silsesquioxane organic moieties), and the second one (350–686 °C) with losses above 11.6%. An important aspect, as shown by Fig. 8, is that up to 515 °C, adsorbed zeolite is more thermally stable. From this temperature on, the decomposition process for the immobilized zeolite follows a higher residual content (5%, probably due to the TiO_2 and SiO_2 additional residues) in relation to the free zeolite.

Owing to the interest in these materials as hosts for an electroactive species it was intended, in this case, to adsorb specific mediator groups to the molecules that would facilitate subsequent applications in electroanalytical chemistry.

For analogy with titanium (IV) oxide adsorbed onto the silica gel surface [30] the resulting material presents too ionic exchange properties. In addition, based on our interest in developing modified electroactive hybrid compounds for electroanalytical purposes, a study concerning electrochemical behavior of Azure A chloride adsorbed on the zeolite modified surface was carried out. Azure A chloride is a cationic phenothiazine compound and it is important in the analytical field for electrocatalysis.

The electrochemical behavior of graphite paste electrode with modified zeolite after Azure A chloride adsorption is demonstrated in Fig. 9 at different scan rates. The cyclic voltammograms of the graphite paste electrode modified showed two redox couples with formal potential ($E^{0\prime}$), where $E^{0\prime} = ((E_{Pa} + E_{Pc})/2$ and E_{Pa} and E_{Pc} are anodic and cathodic potential) at −0.1 and 0.21 V to I and II redox couples ($v = 700\,mV\,s^{-1}$, B–R buffer pH 3.00) *versus* SCE ascribed to a monomer and dimmer of azure, respectively.

Table 2
Physical features of zeolite NH_4USY and modified NH_4USY with titanium (IV) silsesquioxane

Material	Surface area ($m^2\,g^{-1}$)	Pore diameter (nm)	Micropore volume ($cm^3\,g^{-1}$)	Micropore area ($m^2\,g^{-1}$)	External surface area ($m^2\,g^{-1}$)
NH_4USY	581	22.8	0.224	548	33.2
Modified NH_4USY	433	19.7	0.171	413	20.6

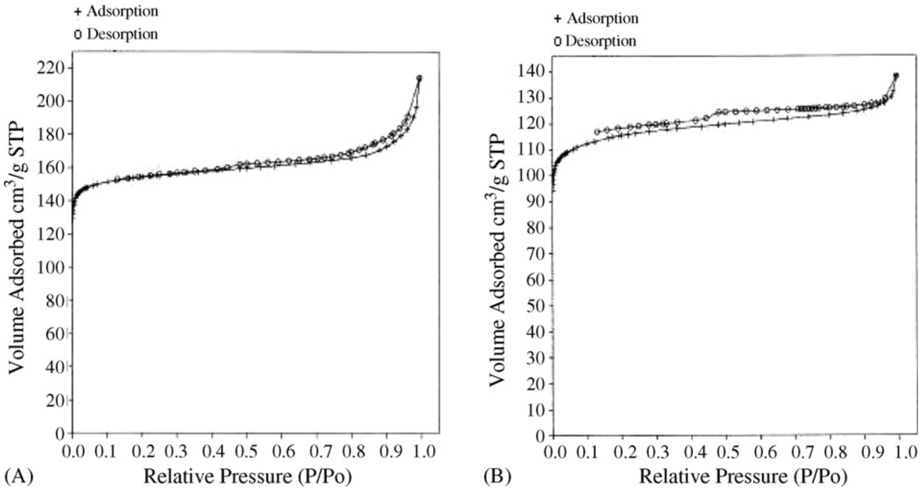

Fig. 7. The isotherms of the zeolite NH_4USY (A); modified zeolite with titanium (IV) silsesquioxane (B).

As depicted in Fig. 9, the electron transfer the electron transfer of Azure A is very fast. In low scan rate (<100 mV s^{-1}) the electron transfer process is not completely clear and the voltmmograms are poor. An excellent linear relationship was verified between the first oxidation peak currents and scan rates from 50 to 700 mV s^{-1} (see graphic inserted in Fig. 9), which is consistent with an effective surface redox process. The separation of the peaks for couple I is about 85 mV, which indeed suggests an adsorptive process [31].

Fig. 10 shows the cyclic voltammograms for a modified graphite paste electrode with zeolite modified after Azure A chloride reaction, in a buffer solution of B–R (pHs 2.00; 3.00; 4.00). The electrochemical parameters are listed in Table 3. The formal potential of both of these redox couples shift linearly in the negative direction with increasing pH solution, also this behaviour is in agreement with the one found for the phenotiazine compounds.

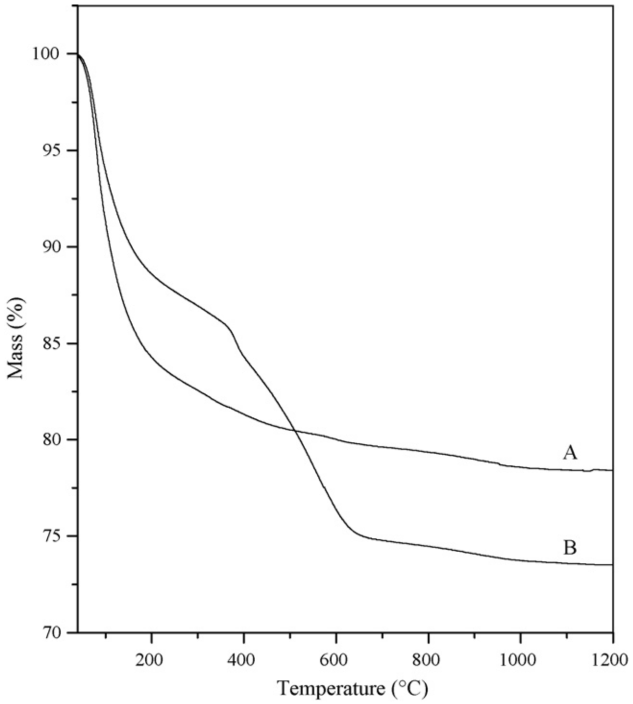

Fig. 8. Thermogravimetric curves for zeolite (A); zeolite containing ([(c-hexil)$_7$Si$_7$O$_9$Ti(OPr^i)] (B) under synthetic air atmosphere.

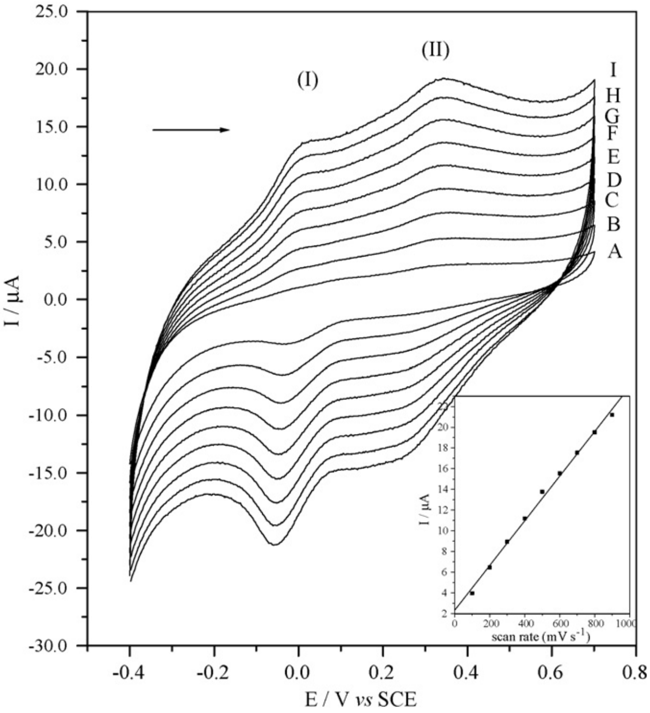

Fig. 9. Cyclic voltammograms of ATZ at different sweep rates: (A) 50 mV s^{-1}; (B) 100 mV s^{-1}; (C) 200 mV s^{-1}; (D) 300 mV s^{-1}; (E) 400 mV s^{-1}; (F) 500 mV s^{-1}; (G) 600 mV s^{-1}; (H) 700 mV s^{-1}; (I) 800 mV s^{-1}; buffer B–R pH 3.0.

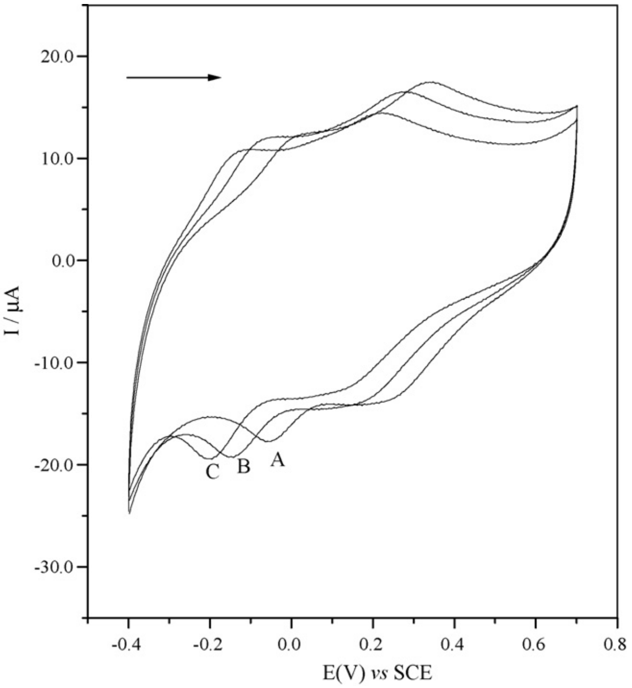

Fig. 10. Cyclics voltammograms of ATZ at differents pH values: (A) pH 2.0; (B) pH 3.0; (C) pH 4.0.

Table 3
Electrochemical parameters of modified graphite paste electrode with ATZ

pH[a]	E_{pa} (V)		E_{pc} (V)		$E^{0\prime}$ (V)		ΔE_p (V)	
	(I)	(II)	(I)	(II)	(I)	(II)	(I)	(II)
2	−0.027	0.343	−0.053	0.223	−0.040	0.283	0.026	0.120
3	−0.058	0.278	−0.143	0.137	−0.100	0.207	0.085	0.141
4	−0.119	0.225	−0.199	0.127	−0.159	0.176	0.080	0.098

$\Delta E_p = E_{pa} - E_{pc}$.

[a] B–R buffer, $\nu = 700\ \text{mV s}^{-1}$.

5. Conclusion

The present work demonstrates that the treatment of NH_4USY zeolite for the extraction of part of the aluminum increases the size of the zeolite pores, facilitating the Ti(IV) silsesquioxane inclusion. In this manner, the Ti(IV) silsesquioxane can be easily encapsulated into the NH_4USY zeolite. There is no need for previous functioning of the zeolite surface. The zeolite modified with Ti(IV)silsesquioxane can adsorb Azure A chloride after chemical treatment with H_3PO_4. The cyclic voltammograms of the graphite paste electrode modified, showed two redox couples with formal potential ($E^{0\prime}$), where $E^{0\prime} = (E_{Pa} + E_{Pc})/2$ −0.1 and 0.21 V to I and II redox couples, respectively ($v = 700\,\text{mV}\,\text{s}^{-1}$; B–R buffer pH 3), *versus* SCE ascribed to a monomer and dimmer of azure. This material is a potential candidate for electroanalytical application.

Acknowledgements

The authors would like to express their gratitude for the financial support by the Fundação de Amparo à Pesquisa do Estado de São Paulo (FAPESP-Proc. 01/04494-0 and 03/12882-6).

References

[1] R.H. Baney, M. Itoh, A. Sakakibara, T. Suzuki, Chem. Rev. 95 (1995) 1409.
[2] M.G. Voronkov, V.L. Lavrent'yev, Top. Curr. Chem. 102 (1982) 199.
[3] H.C.L. Abbenhuis, Chem. Eur. J. 6 (2000) 25.
[4] F.J. Feher, T.A. Budzichowski, Polyhedron 14 (1995) 3239.
[5] P.G. Harrison, R. Kannengiesser, J. Organomet. Chem. 542 (1997) 141.
[6] F.J. Feher, T.L. Tajima, J. Am. Chem. Soc. 116 (1994) 2145.
[7] W.A. Hermann, R. Anwander, V. Dufaud, W. Scherer, Angew. Chem. 106 (1994) 1338.
[8] W.A. Hermann, R. Anwander, V. Dufaud, W. Scherer, Angew. Chem. Int. Ed. Engl. 33 (1994) 1285.
[9] J.-C. Liu, S.R. Wilson, J.R. Shapley, F.J. Feher, Inorg. Chem. 29 (1990) 5138.
[10] I.E. Buys, et al. J. Mol. Catal. 86 (1994) 309.
[11] G.P. Shelud'ko, N.Y. Kuz'menko, N.S. Penkin, V.V. Sukakev, Izobreteniya 4 (1995) 139.
[12] K. Kadama, M. Sugimura, H. Yuda, Japanese Patent 06,271,771.
[13] R. Weidner, N. Zeller, B. Deubzer, V. Frey, US Patent. 5,047,492.
[14] J.D. Lichtenhan, in: J.C. Salamone (Ed.), Polymeric Materials Encyclopedia, CRC Press, 1996, p. 7768.
[15] G.H. Mehl, J.W. Goodby, Angew. Chem., Int. Ed. Eng. 35 (1996) 2641.
[16] M. Moran, C.M. Casado, I. Cuadrado, Organometallics 12 (1993) 4327.
[17] L. Losada, M.P. Garcıa Armada, B. Alonso, B. Gonzalez, C.M. Casado, J. Zhang, J. Organomet. Chem. 689 (2004) 2789.
[18] H. Schimidt, Mater. Res. Soc. Symp. 171 (1990) 3.
[19] S. Kritgen, L. Mojet, H.C.L. Abbenhuis, J.H.C. Van Hoof, R.A. Van Santen, Phys. Chem. Chem. Phys. 1 (1999) 361.
[20] P. Smet, J. Riondato, T. Pauwels, L. Moens, L. Verdonck, Inorg. Chem. Commun. 3 (2000) 557.
[21] F.J. Feher, T.A. Budzichowski, J. Organomet. Chem. 379 (1989) 33.
[22] J.P. Collman, M. Marroco, P. Denisevich, C. Koval, F.C. Anson, J. Electroanal. Chem. 101 (1979) 717.
[23] L. Quian, Z.F. Yan, Colloids Surf. A: Physicochem. Eng. Aspects 180 (2001) 311.
[24] A. Carma, Chem. Rev. 97 (1997) 2372.
[25] L. Frunza, H. Kosslick, H. Landmesser, E. Hoff, R.H. Fricke, J. Mol. Catal. A: Chem. 123 (2–3) (1997) 179.
[26] H. Marsmann, J.P. Kintzinger, Oxigen-17 and Silicon 29 NMR, Springer-verlag, New York, 1981, p. 74.
[27] S.J. Gregg, K.S.W. Sing, Adsorption, Surface Area and Porosity, 2nd ed., Academic, London, 1982.

[28] Pure Appl. Chem. 31 (1978) 578.
[29] S.E. Sen, S.M. Smith, K.A. Sullivan, Tetrahedron 55 (1999) 12657.
[30] A.A.S. Alfaya, Y. Gushikem, S.C. de Castro, Chem. Mater. 10 (1998) 909.
[31] A.J. Bard, L.R. Faulkner, Electrochemical Methods: Fundamentals and Applications, Wiley, New York, 1980.